

Synthesis and characterization of porous 4VP-based adsorbent for Re adsorption as analogue to ^{99}Tc

Pu-Yin Wang¹ · Jian-Hua Zu¹ · Yue-Zhou Wei¹

Received: 23 December 2015 / Revised: 19 April 2016 / Accepted: 21 April 2016 / Published online: 31 January 2017
© Shanghai Institute of Applied Physics, Chinese Academy of Sciences, Chinese Nuclear Society, Science Press China and Springer Science+Business Media Singapore 2017

Abstract Technetium (^{99}Tc), a major fission product in nuclear reactors, of high yield, long-half-life and high mobility in the environment must be removed in nuclear fuel reprocessing. Considering rhenium (Re) and Tc are both VIIB elements, Re is a good chemical analogue to ^{99}Tc . Herein, we use Re as a substitution of ^{99}Tc to study adsorption and desorption behavior. Porous 4-vinylpyridine–divinylbenzene-based (4VP–DVB) adsorbent containing tertiary amine groups is synthesized by suspension polymerization and characterized by BET, TGA, SEM and laser particle size analyzer. The adsorbent has high adsorption efficiency toward Re(VII) in 0.1 mol/L nitric acid solution, and the adsorption equilibrium can be achieved in 30 min. The adsorption kinetics of Re(VII) follows pseudo-second-order rate equation, the adsorption isotherm matches well with the Langmuir isotherm, and the adsorption capacity of Re(VII) on 4VP–DVB adsorbent is 352.1 mg/g at 298 K. Thermodynamic study reveals that the adsorption process is exothermic. This adsorbent is of separation convenience when a fixed-bed column is used, compared to the batch adsorption treatment.

Keywords Rhenium · Technetium · Porous adsorbent · Adsorption

1 Introduction

Technetium-99 (^{99}Tc) is a β^- -emitter with half-life of 2.13×10^5 year. It is a major fission product in nuclear reactors, with fission yield of 6.13% [1]. The ^{99}Tc is known to be co-extracted with uranium during the plutonium and uranium redox extraction (PUREX) process by tributyl phosphate (TBP) [2]. Due to its high yield, long-life and high mobility in the environment, ^{99}Tc must be removed in nuclear fuel reprocessing [3, 4].

Various techniques have been applied to recover ^{99}Tc such as ion exchange, solvent extraction and precipitation [3, 5, 6]. Large amount of secondary waste is generated through precipitation and solvent extraction, which increases the cost of the process. Ion exchange, being easy to operate, with high selectivity, virtually no secondary waste, is an environment-friendly technology. Considering that rhenium (Re) and Tc are both VIIB elements, with the same arrangements of orbital electrons [7], and also the ionic states of both ^{99}Tc and Re in solution and solid are in the most stable oxidation state of +7 (TcO_4^- and ReO_4^-) [8]. Therefore, Re is suitable as a substitution for ^{99}Tc in studying adsorption behavior of ^{99}Tc at high concentrations [4, 9–11]. On the other hand, it is meaningful to study Re, a rare metal used widely in petrochemical industry, aviation, medicine and metallurgy [12–17].

The electrostatic interaction between Re(VII) and the protonated amine groups of the adsorbent is a key factor of the Re(VII) adsorption [11]. Some amine-containing organic polymers have been used to remove ^{99}Tc , such as Amberlite IRA-904 and IRA-900 [18]. Kim et al. used natural materials containing amino groups to separate Re as an analogue to ^{99}Tc [11]. However, the functional groups of the alkylamino-containing adsorbents can be easily

This work was supported by the National Natural Science Foundation of China (Nos. 91226111 and 11675103).

✉ Jian-Hua Zu
zujianhua@sjtu.edu.cn

¹ School of Nuclear Science and Engineering, Shanghai Jiao Tong University, Shanghai 200240, China

damaged under irradiation or in acid. Fortunately, adsorbents which contain pyridine, quinoline, and their derivatives, have showed good irradiation stability [19].

The 4VP–DVB adsorbent containing pyridine exhibits better chemical and irradiation stability than conventional adsorbent [20]. By overcoming disadvantages of bulk polymerization and solution polymerization, suspension polymerization can be realized in production scale. In the synthesis process of 4VP–DVB adsorbent, the pore volume can be adjusted by changing the ratio of cyclohexane and cyclohexanone, where cyclohexane is used as non-solvating diluent and cyclohexanone is used as solvating diluent, respectively. In our study, porous 4VP–DVB adsorbent was synthesized by suspension polymerization. As expected, its exchange rate toward Re(VII) was higher than normal adsorbents. The initial concentration effect of nitric acid, the adsorption kinetic, isotherm and thermodynamic of Re(VII) adsorption on 4VP–DVB were studied in batch experiments. Also, the continuous Re(VII)-adsorption on 4VP–DVB and elution experiment was performed by column experiment.

2 Experimental

2.1 Materials

The 4-vinylpyridine (4VP) stabilized by hydroquinone in purity of 95% and benzoyl peroxide as initiator were purchased from J & K Technology Co. Ltd. Gum arabic powder, cyclohexanone and cyclohexane were obtained from Sino-pharm Chemical Reagent Co. Ltd. K_2ReO_4 in spectroscopical purity and divinylbenzene (DVB, 55%) stabilized with 1000 ppm 4-tert-butylcatechol were purchased from Alfa Aesar. The hydrochloric acid (0.1001 mol/L) and sodium hydroxide solution (0.1025 mol/L) for titration were from Sino-pharm Chemical Reagent Co. Ltd..

2.2 Preparation and characterization of 4VP–DVB adsorbent

Before the synthesis, 4VP inhibitor and divinylbenzene mixture were further purified. By vacuum distillation at 338 K, the polymerization inhibitor in 4VP was removed. The polymerization inhibitor in divinylbenzene (DVB, 55%) mixture was washed off by 5% sodium hydroxide solution, with the DVB left. The organic phase was used in the synthesis process included monomer 4VP (12.5 mL), cross-linking agent DVB (12.5 mL), cyclohexane as non-solvating diluent (8 mL) and cyclohexanone as solvating diluent (18 mL), and benzoyl peroxide as initiator (0.48 g). The aqueous phase was 5 g gum arabic powder as dispersant reagents in 258 mL deionized water. The organic

phase was mixed with the aqueous phase at room temperature. Then, the mixture was stirred at 280 rpm for 8 h at 353 K, with nitrogen atmosphere protection. The adsorbent and liquid phase in the mixture were separated, and the adsorbent was washed successively with hot deionized water, acetone and deionized water. Finally, the adsorbent was vacuum-dried at 313 K for 48 h and porous 4VP–DVB adsorbent was obtained.

The 4VP–DVB adsorbent samples were tested by a surface area and pore size analyzer (Quantachrome: NOVA 2220e). The particle size distribution was obtained by a laser particle size analyzer (Malvern: Mastersizer 3000). Morphology of porous 4VP–DVB adsorbent was characterized by a scanning electron microscope (NOVA Nano-SEM 230). Thermal stability of adsorbent was evaluated by thermogravimetric and differential thermal analysis (TG–DTA, TGA-60, Shimadzu). The nitrogen content contributed by 4-vinylpyridine in 4VP–DVB was determined by titration (Titration Excellence Line T50).

2.3 Batch experiments

In the batch experiments, 0.05 g 4VP–DVB adsorbent mixed with 5 mL aqueous solution was shaken mechanically at 120 rpm at 298 K for a certain period of time. The adsorbent and solution phases were separated by Buchner funnel. The Re contents before and after adsorption were analyzed by inductively coupled plasma atomic emission spectroscopy (ICP–AES: Shimadzu ICPS-7510). All results of the batch experiments were from duplicate tests, with relative errors of about 5%.

The adsorption efficiency (E), adsorption amount (Q) and distribution coefficient (K_d) were calculated as follows

$$E = (C_0 - C_e)/(100C_0), \quad (1)$$

$$Q = (C_0 - C_e)V/m, \quad (2)$$

$$K_d = (C_0 - C_e)V/(mC_e), \quad (3)$$

where C_0 (mg/L) and C_e (mg/L) were Re(VII) initial concentration and equilibrium concentration, respectively; V is volume of the aqueous phase (L); and m is the weight of 4VP–DVB adsorbent (g).

2.4 Column experiments

The batch experiments cannot give accurate scale-up data in dynamic systems. Therefore, the column experiment of 4VP–DVB adsorbent is necessitated. A glass column ($\Phi 5$ mm \times 50 mm) filled with 0.44 g 4VP–DVB adsorbent was used for the removal of Re(VII). Before the test, the adsorbent was treated by nitric acid (50 mL, 1 M) flowing through the column, followed by flowing 0.1 M nitric acid (50 mL) for the purpose of pre-equilibrium.

Finally, column adsorption tests were conducted at 298 K using Re(VII) solution (1000 mg/L) in 0.1 M nitric acid.

Desorption experiment of Re(VII) was carried out under column condition. The 4VP–DVB was loaded with Re(VII) as described above. $\text{NH}_3\cdot\text{H}_2\text{O}$ (25 mL, 1 M), as Re(VII) elution agent, was pumped through the column at a rate of 0.3 mL/min. Fractions were collected, and Re concentration in each fraction was analyzed by ICP–AES. All results were from duplicate tests, and the relative error of column experiments was about 10%.

3 Results and discussion

3.1 Characterization of the prepared adsorbent

The surface area of porous 4VP–DVB adsorbent was $20.4 \text{ m}^2/\text{g}$ according to Brunauer Emmett and Teller method (BET method), and the mean pore diameter was 3.74 nm according to Barrett–Joyner–Halenda method (BJH method). Figure 1a shows the particle size distribution. Most particles were distributed in the range of 40–135 μm , and the average particle size was 75 μm . Surface morphology of the adsorbent is shown in Fig. 1b. The thermal stability of the 4VP–DVB adsorbent was investigated at 293–823 K, with the heating rate of 1 K/min under nitrogen atmosphere. As shown in Fig. 2, the initial decomposition temperature was 557 K, and 85% weight loss occurred at 563–683 K, due to the decomposition of 4-vinylpyridine. The results indicate that the 4VP–DVB adsorbent with pyridyl groups has good thermal stability.

The 4-vinylpyridine in 4VP–DVB reacts with strong acid because of the nitrogen atoms, so content of the functional groups can be determined by titration. Excessive hydrochloric acid (0.1001 mol/L) was reacted with 4VP–

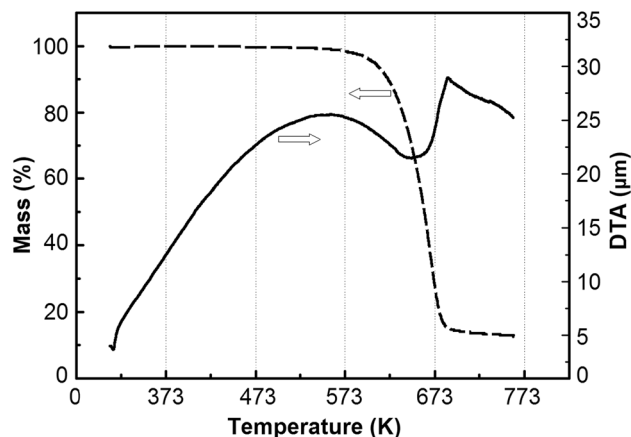


Fig. 2 TG-DTA curves of 4VP–DVB adsorbent

DVB. The left hydrochloric acid in solution was titrated by NaOH solution (0.1025 mol/L) by titrator. The content of nitrogen atoms is 4.02 mmol/g.

3.2 Effect of acidity on adsorption efficiency

The acidity of aqueous solution has significant effect on the adsorption process. Figure 3 shows the Re(VII) adsorption efficiency on 4VP–DVB adsorbent at initial HNO_3 concentrations of 0.1–5 M. The adsorption efficiency decreases with increasing initial HNO_3 concentration. Compared with nitrate and chloride anions, large monovalent anions like TcO_4^- and ReO_4^- with relatively low free energies of hydration can be removed easily from aqueous solution by adsorbents [21]. The process of ion exchange is shown in Fig. 4. However, when the NO_3^- concentration is far greater than ReO_4^- , the completion of NO_3^- with ReO_4^- for the exchange sites on 4VP–DVB adsorbent leads to the decrease in Re(VII) adsorption

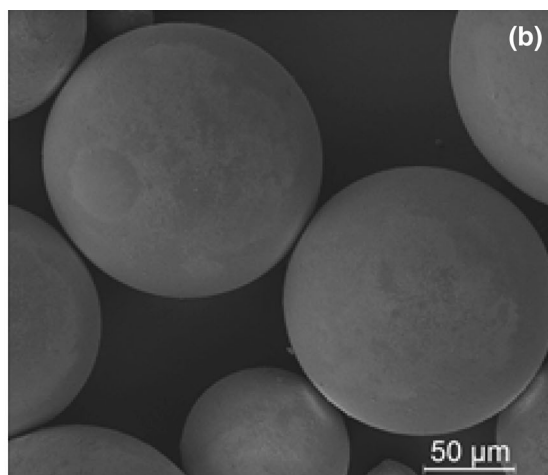
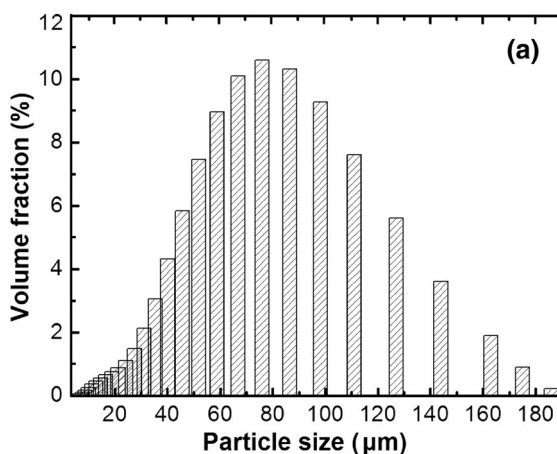


Fig. 1 Particle size distribution (a) and SEM image (b) of the 4VP–DVB adsorbent

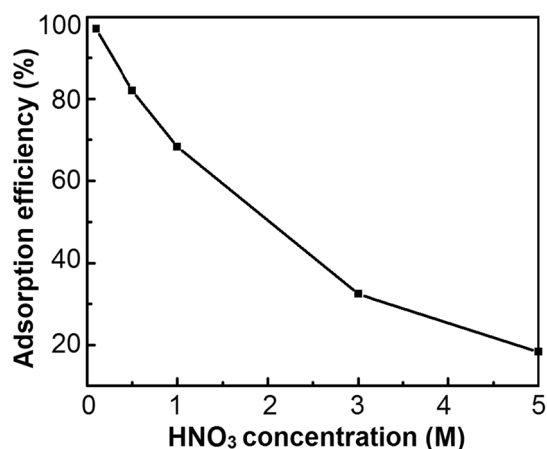


Fig. 3 Effect of HNO₃ concentration on adsorption efficiency of Re(VII)

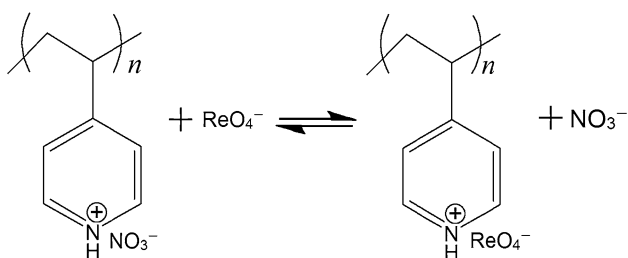


Fig. 4 4VP-DVB ion exchange with perchrenate

efficiency [22]. In general, the 4VP-DVB adsorbent possesses good adaptability as HNO₃ concentration changes.

3.3 Adsorption thermodynamics of Re(VII)

Over the reverse temperature effect on the adsorption efficiency, the adsorption thermodynamic experiments were carried out at 298, 303, 308 and 313 K, each for 24 h. Thermodynamics of Re(VII) adsorption on 4VP-DVB adsorbent was calculated by

$$\ln K_d = \Delta S/R - \Delta H/(RT), \quad (4)$$

where K_d is the distribution coefficient, ΔS is the entropy, ΔH is the enthalpy, T is temperature (K), and $R = 8.13 \text{ J mol}^{-1} \text{ K}^{-1}$ is the universal gas constant. Figure 5 shows the plot of $\ln K_d$ versus $1000/T$. Calculated from the slope and intercept, the ΔH and ΔS were -16.5 kJ/mol and 11.1 J mol K , respectively. The negative ΔH means that the adsorption is an exothermic reaction, and the raising temperature is harmful to the adsorption reaction.

3.4 Adsorption kinetics for Re(VII)

Adsorption kinetics plays an important role in predicting the rate of removing metallic ions from aqueous solutions.

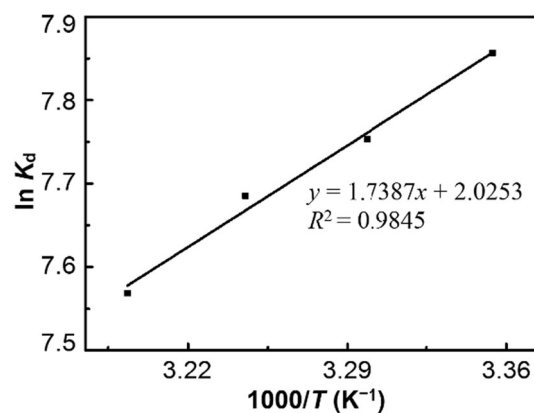


Fig. 5 Plot of $\ln K_d$ versus $1000/T$

The effect of contact time on the adsorption efficiency of ReO_4^- by 4VP-DVB adsorbent is shown in Fig. 6. The adsorption efficiency increases rapidly with time in the first 10 min and then increases slowly (just 0.65% in another 10 min) toward a level of equilibrium. The adsorption process may include two sections: the sorption that increased instantly at initial stages due to rapid attachment of ReO_4^- to the surface of the adsorbent. The second stage was slower, because the adsorption process took place within the network structure of 4VP-DVB adsorbent. However, the Re sorption time was 200 min with the non-porous Purolite A170 weakly alkaline anionite [23]. Therefore, porous 4VP-DVB adsorbent is of high adsorption kinetics.

Pseudo-first-order and pseudo-second-order models were expressed by the following equations, respectively [24, 25]

$$\text{Pseudo-first-order: } \ln(Q_e - Q_t) = \ln Q_e - k_1 t, \quad (5)$$

$$\text{Pseudo-second-order: } t/Q_t = 1/(k_2 Q_e^2) + t/Q_e, \quad (6)$$

where Q_e and Q_t are the amount of Re(VII) adsorbed on adsorbent (mg/g) at equilibrium and at time t (min), and k_1 (1/min) and k_2 (g/mg/min) are the rate constants of first-order adsorption and second-order adsorption, respectively.

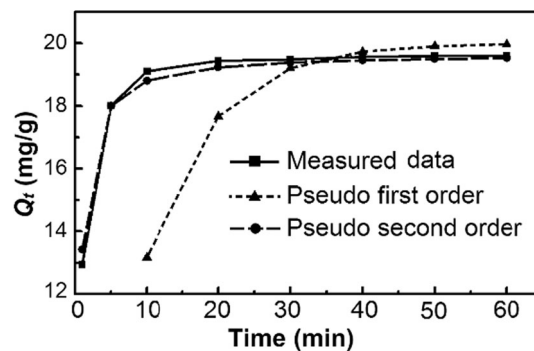


Fig. 6 Kinetic models for Re(VII) adsorption on 4VP-DVB

Plots of Q_t against t for pseudo-first-order and pseudo-second-order models are shown in Fig. 6. The correlation for pseudo-second-order adsorption model (0.989) is higher than that for pseudo-first-order model (0.909). And the adsorption capacities calculated by the pseudo-second-order model are close to the measured data. Therefore, the rate-determining step of the adsorption by 4VP–DVB adsorbent is decided by chemisorption, as the pseudo-second-order adsorption model is based on the assumption that chemisorption is the rate-determining step of adsorption process [26].

3.5 Adsorption isotherm models of Re(VII)

The effect of initial Re(VII) concentration on adsorption of 4VP–DVB was investigated at Re(VII) concentrations of 200–4000 mg/L. The results are shown in Fig. 7. With increasing initial Re(VII) concentrations, the adsorbed Re(VII) at equilibrium (Q_e) increased, but the adsorption efficiency decreased. At high initial Re(VII) concentrations, a higher concentration gradient may exist between 4VP–DVB/solution interface, which ultimately causes higher Re(VII) uptake.

Adsorption isotherm was important to understand the adsorption performance. The Langmuir and Freundlich models have been used by many groups [27–30]. To find out the parameters associated with Re(VII) adsorption, the measured data were analyzed by the two models. The Langmuir and Freundlich isotherms can be described by Eqs. (7, 8) [31].

$$\text{Langmuir equation : } C_e/Q_e = C_e/Q_m + 1/(bQ_m), \quad (7)$$

$$\text{Freundlich equation: } \ln Q_e = \ln K + \ln C_e/n, \quad (8)$$

where Q_e is the adsorption amount at equilibrium (mg/g), C_e is the equilibrium concentration in solution (mg/L), and Q_m is the maximum adsorption capacity, where K and n are the Freundlich constants which relate to the adsorption capacity and the adsorption intensity, respectively. And

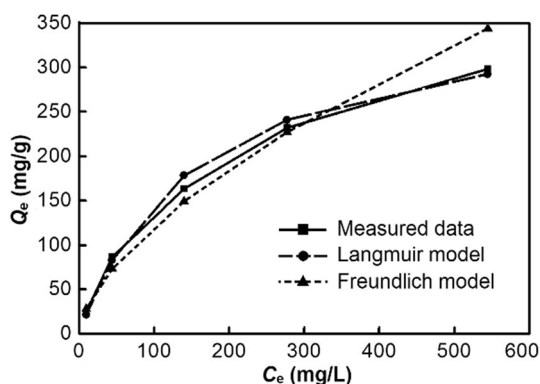


Fig. 7 Adsorption isotherms of Re(VII)

b (L/mg) is Langmuir adsorption constant related to the adsorption affinity.

The Langmuir and Freundlich constants, Q_m and n , were obtained from slopes and intercepts of plots (Langmuir plot: C_e/Q_e vs. C_e and Freundlich plot: C_e and $\ln Q_e$ vs. $\ln C_e$). As shown in Fig. 7, the Langmuir model is better than Freundlich model in fitting the measured data. Calculated by the Langmuir model, the maximum adsorption capacity is $Q_m = 352.1$ mg/g. The value of n was 1.6, which indicated that the adsorption of Re(VII) was a facile process. High values of regression coefficients between the sorbate and sorbent systems for both Langmuir and Freundlich models indicated the applicability of 4VP–DVB adsorbent system for Re(VII) removal in both monolayer sorption and heterogeneous surface conditions.

3.6 Column test

In this test, the results from batch experiments of Re(VII) adsorption were used. A 98% breakthrough occurred at 150 bed volumes. Column capacity calculated from the breakthrough curve was 321 mg/g. The four-cycle breakthrough curves are shown in Fig. 8. The adsorption performance was perfect. The column lost about 3% capacity after the first run and 3–8% after four runs. Therefore, the column can be used for at least 10 runs without any problem. This is economical and would reduce much radioactive waste if 4VP–DVB is used for ^{99}Tc removal.

Regeneration of the adsorbents and recovery of the ^{99}Tc (VII) are important for nuclear wastewater treatment. We used Re(VII) in substitution for ^{99}Tc (VII) to study the desorption behavior. The eluent was 1 M ammonium hydroxide, which can react quickly with H^+ on 4VP–DVB adsorbent, and can be removed easily by heating. As shown in Fig. 9, 10 mL of $\text{NH}_3 \cdot \text{H}_2\text{O}$ was sufficient for desorption of almost all the Re(VII). After 96% of adsorbed Re(VII) was desorbed, the column was washed by 50 mL deionized

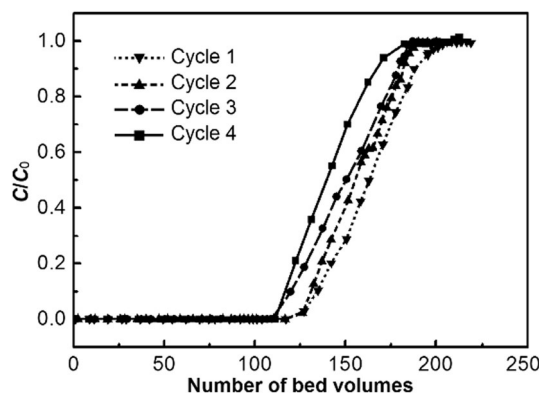


Fig. 8 Breakthrough curves of Re(VII)

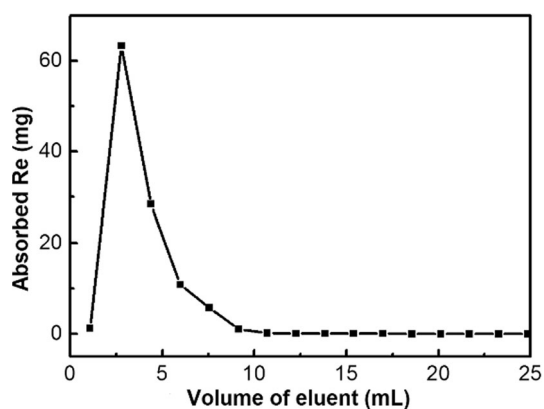


Fig. 9 Desorption of Re(VII) by ammonia (1 M)

water, 50 mL nitrate (1 M) and 50 mL nitrate (0.1 M). The loaded 4VP–DVB adsorbent was regenerated for next use. From the breakthrough curve, the Re(VII) concentration in the desorption solution was ten times of the initial concentration. So, in the column tests, 4VP–DVB adsorbent could reduce waste greatly.

4 Conclusion

The adsorption of Re(VII) was investigated by using porous 4VP–DVB adsorbent prepared through suspension polymerization. The average bead size was 75 μm . The thermal stability of the 4VP–DVB adsorbent was investigated, and the initial decomposition temperature was 557 K. At 0.1 M nitric acid, adsorption reached equilibrium within 30 min and the maximum adsorption capacity for Re(VII) was 352.1 mg/g. Adsorption kinetics was well matched with pseudo-second-order model. The adsorption process follows both Langmuir and Freundlich models, but Langmuir model fitted better the experimental data. The adsorption process was found to be exothermic in nature and ReO_4^- was adsorbed by the adsorbent up to 96–98%. Re(VII) in 150 bed volumes adsorbed by 4VP–DVB adsorbent was eluted from the column using 1 M ammonia in about 11 bed volumes, then Re(VII) was concentrated 10 times. Therefore, it can be concluded that 4VP–DVB adsorbent is an excellent adsorbent and can be used to remove and concentrate Re(VII). Furthermore, all obtained results will provide reference for Tc (VII) removal.

References

1. K. Lieser, Technetium in the nuclear fuel cycle, in medicine and in the environment. *Radiochim. Acta* **63**, 5–8 (1993). doi:10.1524/ract.1993.63.special-issue.5

2. F. Macásek, J. Kadrabova, Extraction of pertechnetate anion as a ligand in metal complexes with tributylphosphate. *J. Radioanal. Chem.* **51**, 97–106 (1979). doi:10.1007/BF02519927
3. G.D. Jarvinen, K.M. Long, G.S. Goff et al., Separation of pertechnetate from uranium in a simulated urex processing solution using anion exchange extraction chromatography. *Solvent Extr. Ion Exch.* **31**, 416–429 (2013). doi:10.1080/07366299.2013.800434
4. R.S. Masud, Y.Y. Wu, H. Mimura et al., Selective separation of Re(VII) and TC(VII) by xerogel microcapsules enclosing TOA extractant. *Procedia Chem.* **7**, 258–267 (2012). doi:10.1016/j.proche.2012.10.042
5. I.A. Shkrob, T.W. Marin, D.C. Stepinski et al., Extraction and reductive stripping of pertechnetate from spent nuclear fuel waste streams. *Sep. Sci. Technol.* **46**, 357–368 (2011). doi:10.1080/01496395.2010.527893
6. T.A. Boitsova, V.A. Babain, A.A. Murzin et al., Precipitation of pertechnetate ion from nitric acid solutions using complexes of copper (II) with heterocyclic *N*-donor ligands. *J. Radioanal. Nucl. Chem.* **307**, 1519–1527 (2016). doi:10.1007/s10967-015-4300-5
7. E. Deutsch, K. Libson, J.-L. Vanderheyden et al., The chemistry of rhenium and technetium as related to the use of isotopes of these elements in therapeutic and diagnostic nuclear medicine. *Int. J. Radiat. Appl. Instrum. Part B Nucl. Med. Biol.* **13**, 465–477 (1986). doi:10.1016/0883-2897(86)90027-9
8. J.G. Darab, P.A. Smith, Chemistry of technetium and rhenium species during low-level radioactive waste vitrification. *Chem. Mater.* **8**, 1004–1021 (1996). doi:10.1021/cm950418+
9. U. Abram, R. Alberto, Technetium and rhenium: coordination chemistry and nuclear medical applications. *J. Braz. Chem. Soc.* **17**, 1486–1500 (2006). doi:10.1590/S0103-50532006000800004
10. H. Braband, T.I. Kückmann, U. Abram, Rhenium and technetium complexes with *n*-heterocyclic carbenes—a review. *J. Organomet. Chem.* **690**, 5421–5429 (2005). doi:10.1016/j.jorganchem.2005.07.014
11. E. Kim, M.F. Benedetti, J. Boulègue, Removal of dissolved rhenium by sorption onto organic polymers: study of rhenium as an analogue of radioactive technetium. *Water Res.* **38**, 448–454 (2004). doi:10.1016/j.watres.2003.09.033
12. W.-C. Hsu, C.-N. Cheng, T.-W. Lee et al., Cytotoxic effects of pegylated anti-EGFR immunoliposomes combined with doxorubicin and rhenium-188 against cancer cells. *Anticancer Res.* **35**, 4777–4788 (2015)
13. E. Fernandez, G. Rodriguez, S. Hostachy et al., A rhenium tris-carbonyl derivative as a model molecule for incorporation into phospholipid assemblies for skin applications. *Colloids Surf. B Biointerfaces* **131**, 102–107 (2015). doi:10.1016/j.colsurfb.2015.04.045
14. P. Collery, A. Mohsen, A. Kermagoret et al., Antitumor activity of a rhenium (I)-diselenoether complex in experimental models of human breast cancer. *Invest. New Drug.* **33**, 848–860 (2015). doi:10.1007/s10637-015-0265-z
15. G. Balakrishnan, T. Rajendran, K.S. Murugan et al., Interaction of rhenium(I) complex carrying long alkyl chain with calf thymus DNA: cytotoxic and cell imaging studies. *Inorg. Chim. Acta* **434**, 51–59 (2015). doi:10.1016/j.ica.2015.04.036
16. S. Verma, S. Kumar, E. Shawat et al., Carbon nanofibers decorated with oxo-rhenium complexes: highly efficient heterogeneous catalyst for oxidation of amines with hydrogen peroxide. *J. Mol. Catal. A Chem.* **402**, 46–52 (2015). doi:10.1016/j.molcata.2015.03.007
17. Y. Xiong, Solubility and speciation of rhenium in anoxic environments at ambient temperature and applications to the black sea. *Deep Sea Res. Part I* **50**, 681–690 (2003). doi:10.1016/S0967-0637(03)00037-2

18. B. Gu, G.M. Brown, P.V. Bonnesen et al., Development of novel bifunctional anion-exchange resins with improved selectivity for pertechnetate sorption from contaminated groundwater. *Environ. Sci. Technol.* **34**, 1075–1080 (2000). doi:[10.1021/es990951g](https://doi.org/10.1021/es990951g)
19. K. Pillay, A review of the radiation stability of ion exchange materials. *J. Radioanal. Nucl. Chem.* **102**, 247–268 (1986). doi:[10.1007/BF02037966](https://doi.org/10.1007/BF02037966)
20. H.R. Obermoller, D.A. White, S. Lagos, Resin adsorption of anionic chloride complexes for uranium isotope chemical exchange reactions. *Hydrometallurgy* **27**, 63–74 (1991). doi:[10.1016/0304-386X\(91\)90078-Z](https://doi.org/10.1016/0304-386X(91)90078-Z)
21. B. Moyer, P. Bonnesen, *Physical Factors in Anion Separations* (Wiley-VCH, New York, 1997)
22. T. Suzuki, Y. Fujii, W. Yan et al., Adsorption behavior of vii group elements on tertiary pyridine resin in hydrochloric acid solution. *J. Radioanal. Nucl. Chem.* **282**, 641–644 (2009). doi:[10.1007/s10967-009-0165-9](https://doi.org/10.1007/s10967-009-0165-9)
23. S. Zakhar'yan, E. Gedgagov, Anion-exchange separation of rhenium and selenium in schemes for obtaining ammonium perchlorate. *Theor. Found. Chem. Eng.* **47**, 637–643 (2013). doi:[10.1134/S0040579513050138](https://doi.org/10.1134/S0040579513050138)
24. Y.-S. Ho, G. McKay, The kinetics of sorption of divalent metal ions onto sphagnum moss peat. *Water Res.* **34**, 735–742 (2000). doi:[10.1016/S0043-1354\(99\)00232-8](https://doi.org/10.1016/S0043-1354(99)00232-8)
25. W. Rudzinski, W. Plazinski, Kinetics of solute adsorption at solid/solution interfaces: a theoretical development of the empirical pseudo-first and pseudo-second order kinetic rate equations, based on applying the statistical rate theory of interfacial transport. *J. Phys. Chem. B* **110**, 16514–16525 (2006). doi:[10.1021/jp061779n](https://doi.org/10.1021/jp061779n)
26. M. Hanafiah, H. Zakaria, W.W. Ngah, Preparation, characterization, and adsorption behavior of Cu (II) ions onto alkali-treated weed (*imperata cylindrica*) leaf powder. *Water Air Soil Pollut.* **201**, 43–53 (2009). doi:[10.1007/s11270-008-9926-2](https://doi.org/10.1007/s11270-008-9926-2)
27. T.M. Ting, M.M. Nasef, K. Hashim, Evaluation of boron adsorption on new radiation grafted fibrous adsorbent containing *n*-methyl-D-glucamine. *J. Chem. Technol. Biotechnol.* (2015). doi:[10.1002/jctb.4793](https://doi.org/10.1002/jctb.4793)
28. V.K. Gupta, A. Rastogi, A. Nayak, Adsorption studies on the removal of hexavalent chromium from aqueous solution using a low cost fertilizer industry waste material. *J. Colloid Interface Sci.* **342**, 135–141 (2010). doi:[10.1016/j.jcis.2009.09.065](https://doi.org/10.1016/j.jcis.2009.09.065)
29. S. Karaca, A. Gürses, M. Ejder et al., Adsorptive removal of phosphate from aqueous solutions using raw and calcinated dolomite. *J. Hazard. Mater.* **128**, 273–279 (2006). doi:[10.1016/j.jhazmat.2005.08.003](https://doi.org/10.1016/j.jhazmat.2005.08.003)
30. T. Anirudhan, P. Radhakrishnan, Improved performance of a biomaterial-based cation exchanger for the adsorption of Uranium (VI) from water and nuclear industry wastewater. *J. Environ. Radioact.* **100**, 250–257 (2009). doi:[10.1016/j.jenvrad.2008.12.006](https://doi.org/10.1016/j.jenvrad.2008.12.006)
31. G. Crini, H.N. Peindy, F. Gimbert et al., Removal of CI basic green 4 (malachite green) from aqueous solutions by adsorption using cyclodextrin-based adsorbent: kinetic and equilibrium studies. *Sep. Purif. Technol.* **53**, 97–110 (2007). doi:[10.1016/j.seppur.2006.06.018](https://doi.org/10.1016/j.seppur.2006.06.018)